

# Absorption dips in Cygnus X-1

Eckhard Strobel  
supervised by:  
Prof. Dr. Jörn Wilms  
Manfred Hanke

April 26, 2010

We present the result of a study of the absorption dips in Cyg X-1 with data from RXTE. The purpose was to find a method to find dips automatically. This was accomplished with a local criterion based on the hardness ratio which characterizes dips in the hard state. With the help of this a dip distribution with respect to orbital phase was gained. It showed that dips are most frequent during superior conjunction of the black hole. In contrast to earlier investigations no dips were found around orbital period  $\phi \sim 0.5$  which is due to the new local criterion. Further we report a temporal evolution in the dip distribution which cannot be due to faults in the ephemeris. Moreover a distribution of the dip length was measured showing that long dips are less frequent than shorter ones.

## Contents

<b>1</b>	<b>Introduction</b>	<b>2</b>
1.1	Cygnus X-1 . . . . .	2
1.2	Dips . . . . .	2
<b>2</b>	<b>Analysis</b>	<b>3</b>
2.1	Data . . . . .	3
2.2	Distinction between hard and soft state . . . . .	4
2.3	Dip characterization . . . . .	4
<b>3</b>	<b>Results</b>	<b>7</b>
3.1	Dip distribution . . . . .	7
3.2	Temporal evolution . . . . .	9
3.3	Length distribution . . . . .	11
<b>4</b>	<b>Summary and outlook</b>	<b>12</b>

# 1 Introduction

## 1.1 Cygnus X-1

Cygnus X-1 is a well studied high-mass X-Ray binary which consist of the O9.7 supergiant HDE 226868 and a compact object with a mass of  $(8.7 \pm 0.8)M_{\odot}$  (Shaposhnikov & Titarchuk, 2007). Due to accretion of mass from the companion on the compact object it is one of the brightest known X-Ray sources. The system shows large variability over a great range of time scales. First of all there are the soft and the hard state. While Cyg X-1 is most time in the hard state in which the luminosity is lower. There were transitions on a monthly time scale, e.g., in 1996 May, into a high luminosity state with a softer spectrum. On short time scales it is also very variable.

## 1.2 Dips

The observed X-Ray emission of Cyg X-1 contains dips. Kitamoto et al. (1984) found the K-absorption-edge of iron in the spectrum of those dips and that during a dip the emitted radiation becomes harder. This leads to the conclusion that the dips are due to photoelectric absorption.

First it was thought that dips occur only during or near superior conjunction of the black hole. But as the distribution of such dips with orbital phase was investigated by Bałucińska-Church et al. (2000) with the help of the RXTE All Sky Monitor the result was that there are two peaks: one at orbital phase  $\phi \sim 0.95$  and one at  $\phi \sim 0.6$ . The second was attributed to an accretion stream from the companion. These authors also explained the different spectra of dips by partial covering of the source and made some connection to the stellar wind in the system.

Poutanen et al. (2008) repeated this study also using data taken after 2000 but this time they did not find an indication for a peak 0.6 which then was claimed to be due to statistical fluctuations.

This work uses the monitoring data from pointed observations with the Proportional Counter Array (PCA) of RXTE with a much better time resolution to improve the statistics of the dips. A criterion is developed to find automatically dips in the hard state. From these a distribution over the orbital period is gained. The data are also sufficient to see a temporal evolution in the dip distribution. In addition a distribution of dip length can be measured due to the good time resolution. This distribution could be helpful information for further understanding of the causes of dipping in Cyg X-1.

## 2 Analysis

### 2.1 Data

The data used here are from several observations of Cyg X-1 with the Proportional Counter Array (PCA) of the Rossi X-ray Timing Explorer (RXTE) from 1996 October 23 till 2010 January 14 with a time resolution of 0.125s. Fig. 1 shows the observation time per month for the hole time span. The data were split at gaps longer than 10min into a total number of 1531 intervals. The RXTE is in an 600km orbit around Earth and has a period of 90min. Most datasets therefore have an duration of approximately 50min due to covering of the source by Earth. The used channels can be seen in Table 1. The energy spans are not accurate since they changed during so called calibration epochs (see Jahoda et al., 2006). For the characterization of the dips a hardness ratio was used, which is calculated as  $(\text{rate}_5 + \text{rate}_6 + \text{rate}_7 + \text{rate}_8) / (\text{rate}_1 + \text{rate}_2)$  corresponding to  $(8.3 - 14.9 \text{keV}) / (0 - 5.8 \text{keV})$  and from now on denoted as the hardness ratio. The energy bands were chosen such that they have approximately the same count rates in the hard state and thus statistical quality.

Table 1: Used PCA-channels and corresponding energy in PCA calibration epoch 5 <sup>1</sup>

energy band	1	2	3	4	5	6	7	8
PCA channels	0-10	11-13	14-16	17-19	20-22	23-26	27-30	31-35
max energy in keV	4.5	5.7	7.0	8.2	9.5	11.1	12.8	14.8

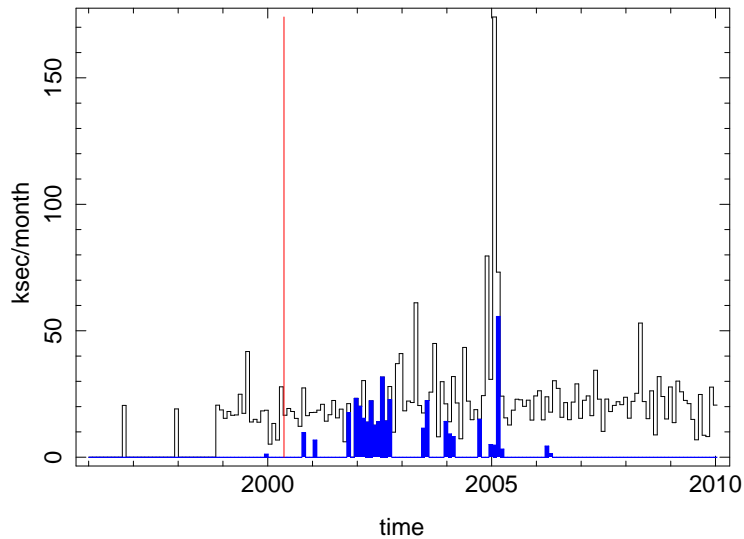


Figure 1: Monthly exposure. The blue parts correspond the observations classified as soft state which were excluded for analysis. The red line shows the beginning of the PCA calibration epoch 5.

<sup>1</sup>see [http://heasarc.gsfc.nasa.gov/docs/xte/e-c\\_table.html](http://heasarc.gsfc.nasa.gov/docs/xte/e-c_table.html)

## 2.2 Distinction between hard and soft state

As Cyg X-1 has different states (for a more intensive discussion see Remillard & McClintock, 2006) it was important to categorize the data according to their state. To distinguish between hard and soft state a hardness-intensity-diagram was obtained. Therefore for each dataset a mean value of the hardness ratio is plotted against the mean value of the softest energy band. In Fig. 2 one can distinguish between the hard/low luminosity and the soft/high luminosity states. For the sake of simplicity the data were counted as in the soft state if the hardness ratio was smaller than 0.3. The blue parts in Fig. 1 show which parts of the observation satisfy this condition.

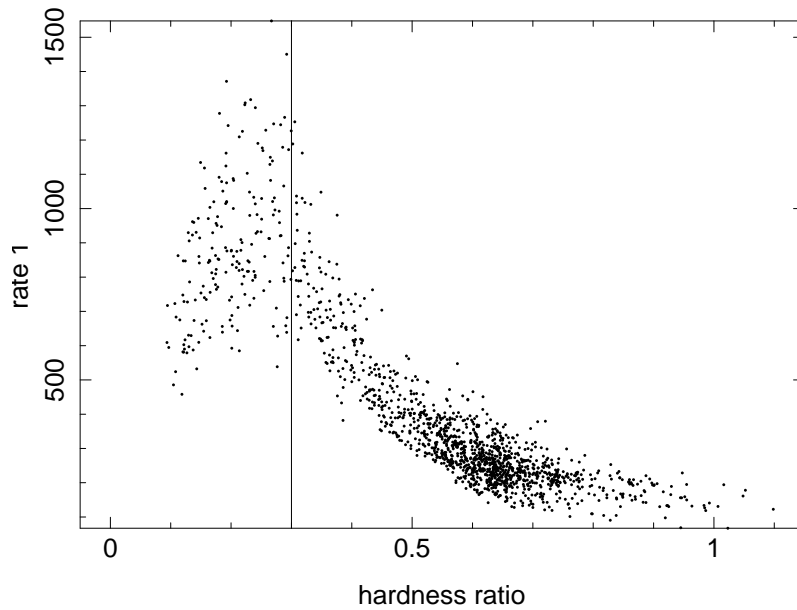


Figure 2: Hardness-intensity-diagram. The vertical line shows how soft and hard states were categorized.

## 2.3 Dip characterization

Because of the intrinsic variability of the source it is not easy to characterize dips in the light curves. To find absorption dips it is convenient to characterize dips according to an increase in the sources hardness. In previous works mostly a fixed limit for the hardness ratio was used (Bałucińska-Church et al., 2000; Poutanen et al., 2008).

Due to the intrinsic variability of the source, it seems to be more convincing to set a local criterion. Therefore the mean values  $\mu$  and standard deviation  $\sigma$  of the hardness ratio were calculated for each data set. A time span is characterized as a dipping event if its hardness ratio lies  $2\sigma$  over the mean value. To smooth out local fluctuations and so characterize the length of dips in a better way, a moving average over 7 data points (0,875s) was used instead of the hardness ratio itself. This seemed to give a more natural distinction of long dips which otherwise were split in to several smaller ones. As this method tends to characterize local fluctuations as dips, only structures with durations longer than 1 s were counted as dips.

Fig. 3 shows a typical dip in the hard state. The characteristics of an absorption dip are clearly visible. The count rate in the soft energy band decreases rapidly whereas the hard one stays almost constant. The plot also shows the criterion which is used to identify the dips (i.e., moving mean of hardness ratio  $-\mu - 2\sigma$ ) and the hardness ratio.

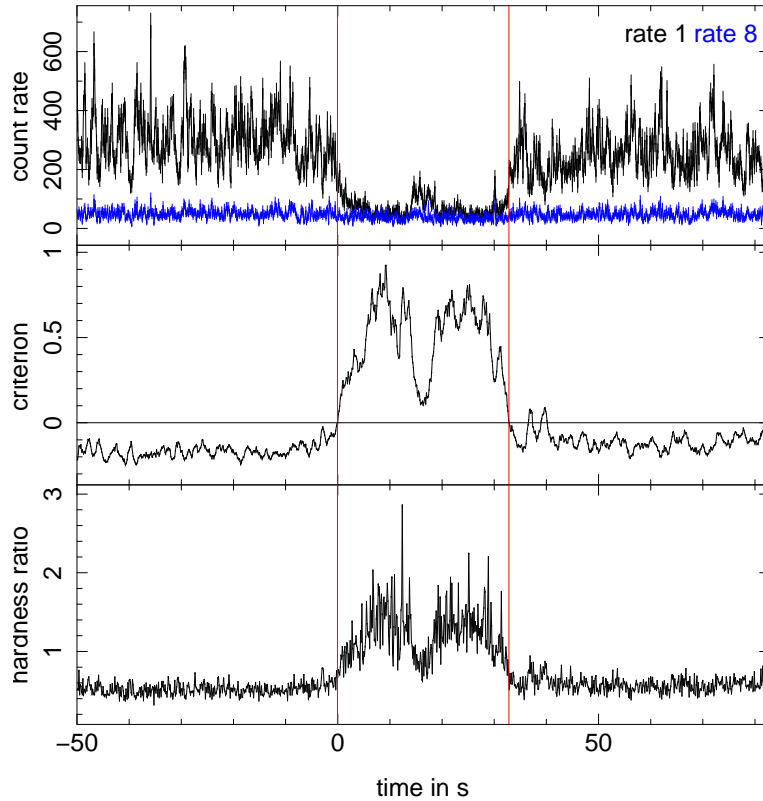


Figure 3: Typical dipping event in the hard state. Count rate in soft (rate1) and hard (rate8) band (top), criterion for dip selection (middle) and hardness ratio (bottom).

Fig. 4 shows what is typically characterized as dip in the soft state. Unlike in the hard state case this event does not show the characteristics of an absorption dip. The increase in the hardness ratio shows a longer timescale trend. Moreover the count rate is not decreasing but increasing. Almost all "dipping" events in the soft state show this correlation between count rate and hardness ratio which is typical for soft state variability. This behavior is also visible in the hardness-intensity-diagram (see Fig. 2). So because of the higher variability the criterion is obviously not characteristic for dips in the soft state.

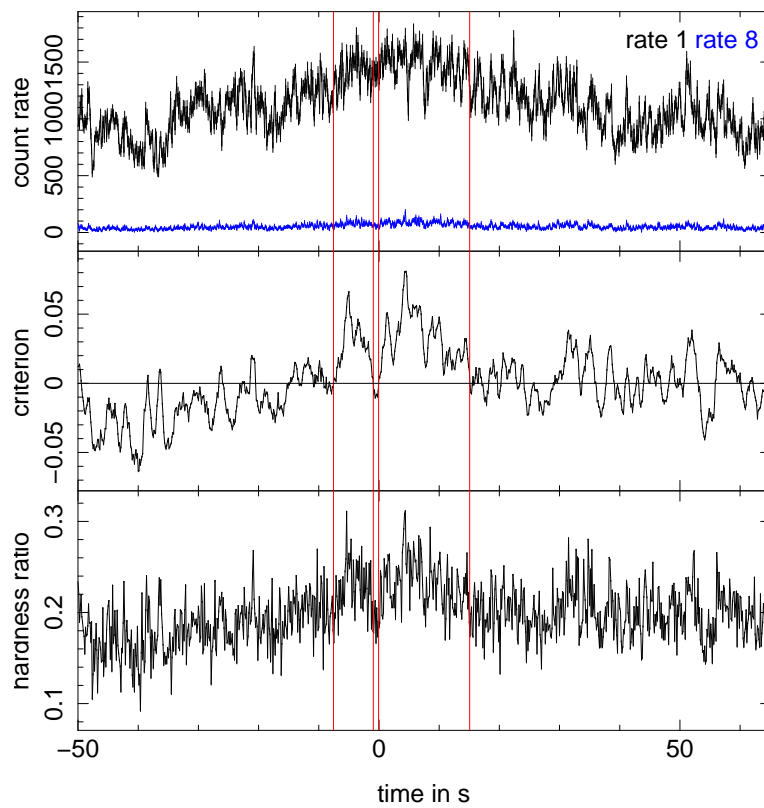


Figure 4: Typical dipping event in the soft state. Count rate in soft (rate 1) and hard (rate 8) band (top), criterion for dip selection (middle) and hardness ratio (bottom).

## 3 Results

### 3.1 Dip distribution

Using the criterion described in section 2.3, 3154 dipoles were found in the whole data set. Only 857 of them were in the hard state. This is contradictory to the results of Poutanen et al. (2008) who found a larger number of dipoles in the hard state. This is clear because of their fixed threshold in the hardness ratio for dip characterization. But as discussed beforehand, our criterion is only working in the hard state. Therefore only the dipping events in hard state are discussed in this work from now on.

To gain a distribution of the dipoles with respect to orbital phase the orbital period was divided into 20 bins. To avoid selection effects each phase bin was normalized with the exposure in the phase bin. Fig. 5 shows the result. There is a clear maximum at orbital phase  $\phi \sim 1.0$  which is consistent with the earlier observations of Bałucińska-Church et al. (2000) and Poutanen et al. (2008). The difference is that around orbital phase  $\phi \sim 0.5$  no dipoles are found at all, while the earlier investigations always seemed to find a background or even the peak at  $\phi \sim 0.6$ . The reason for this difference lies in our criterion which in contrast to the earlier ones takes local long time fluctuations into account.

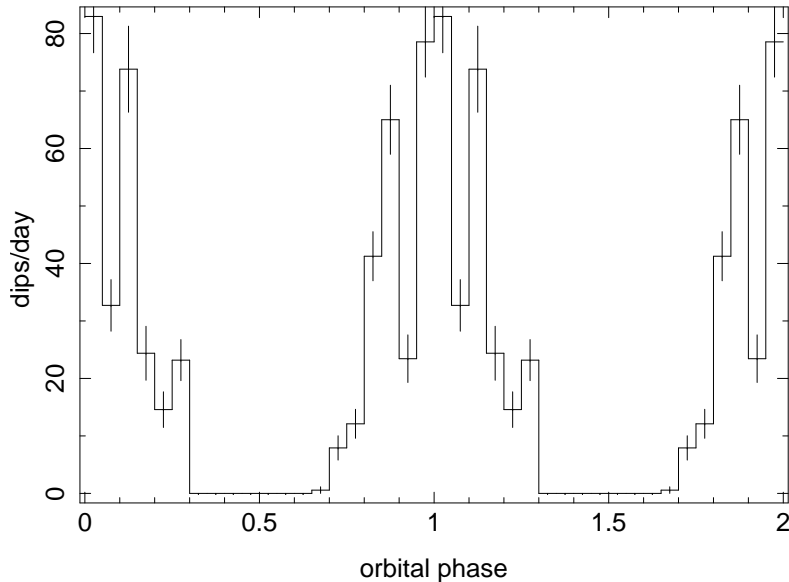


Figure 5: Distribution of the hard dipoles over the orbital period

To test the statistical stability of the dip distribution, several subsets of the data were taken and compared. Fig. 6 shows the distribution subsets of even and odd observation numbers, while Fig. 7 shows the first and second half of the whole campaign.

For the first division the distribution seems to be stable. This leads to the assumption that the peaks around  $\phi \sim 1.0$  are no statistical effects. In fact the second subsets show that the dip distribution seems to differ with time as there is much difference between the first and the second time span of the observation.

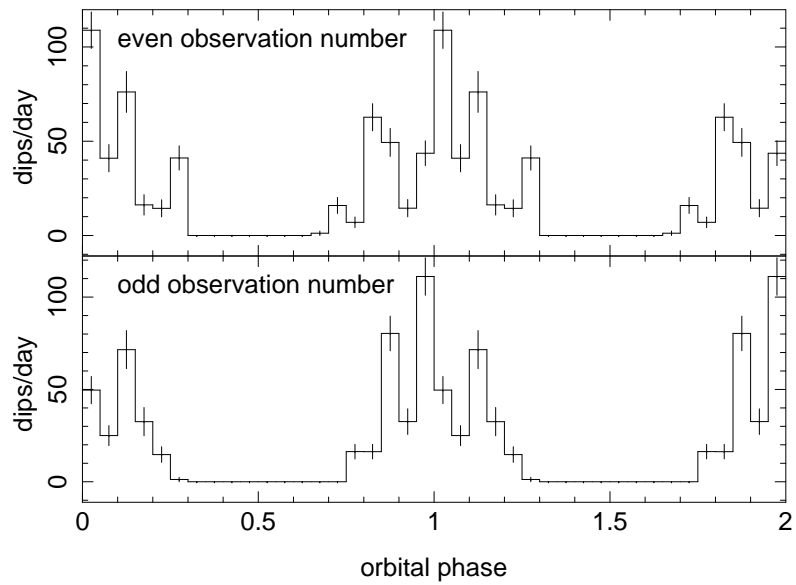


Figure 6: Subsets of the dip distribution using every other dataset

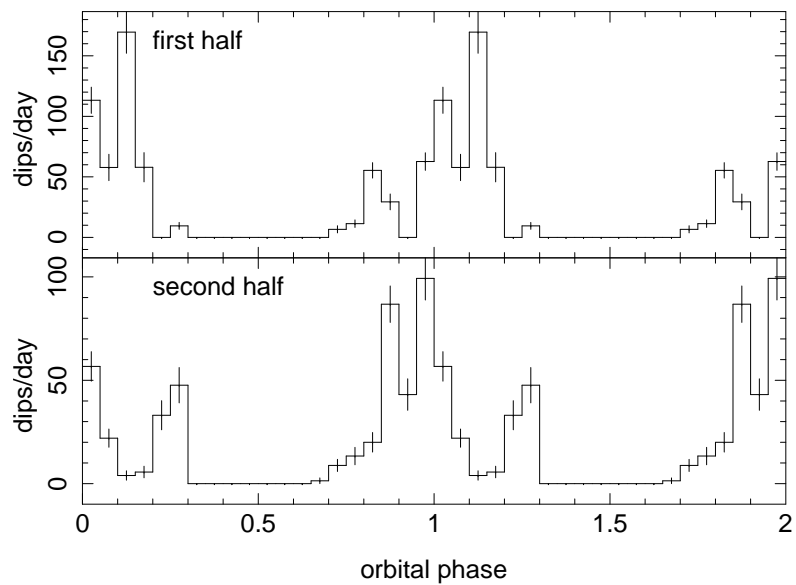


Figure 7: Subsets of the dip distribution using the first and second half of the campaign

### 3.2 Temporal evolution

The evolution of the dip distribution in time was examined further by dividing the observations into smaller bits. This is only possible to certain minimal size for a subset because the statistic is affected if the number of observations in one of the phase bins reaches zero. To see a temporal trend it is important that the subsets are connected. Because of the beginning of regular monitoring in 1999 and the long soft state in 2002, the first time span was given "naturally". The remaining intervals were chosen by starting after the soft state and splitting the data in subsets with approximately the same exposure as the first one. This results in the four time spans seen in Table 2.

Table 2: Duration of the four intervals

interval	1	2	3	4
time in MJD	51192–52216	52553–53329	53329–53897	52897–54666

Fig 8 shows the corresponding dip distributions. The orbital distribution of dips is clearly shifting in time. It is unlikely that this is due to faults in the ephemeris because this would only result in shifting into one direction whereas the phase bin with the most dips seems to shift in negative direction from interval 2 to 3 but in positive from interval 3 to 4.

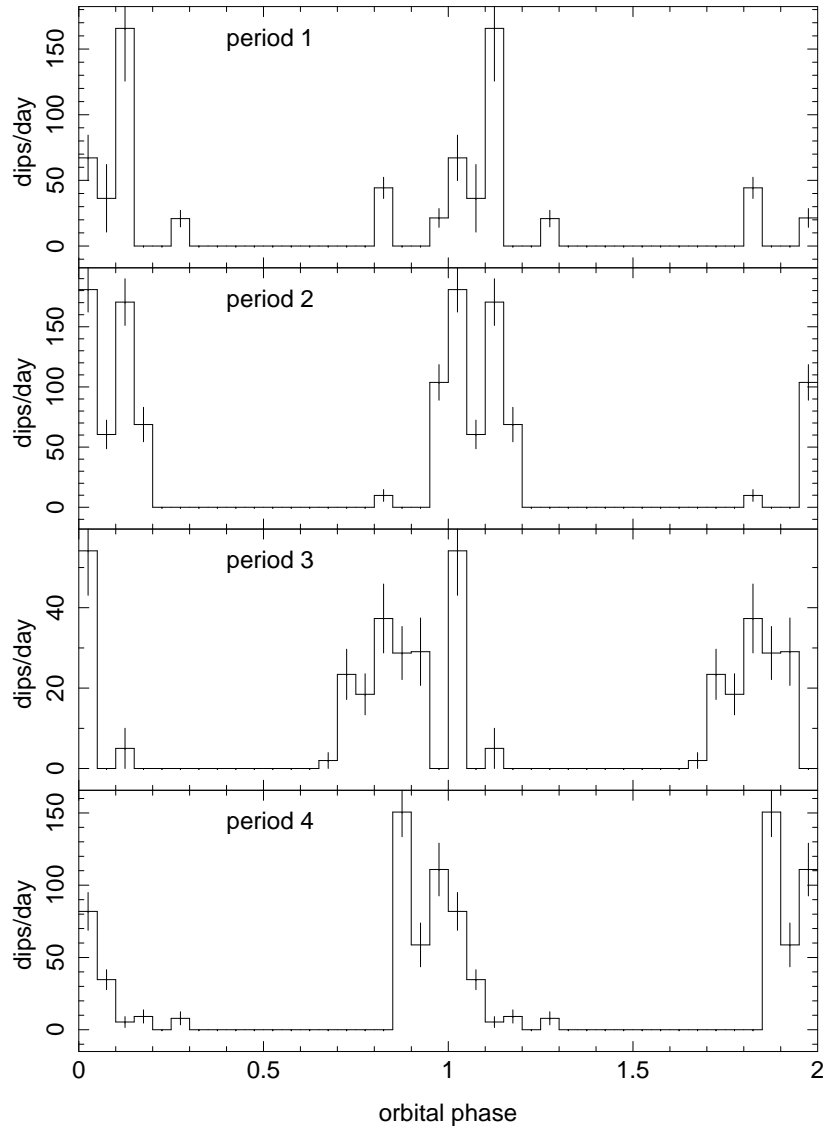


Figure 8: Temporal evolution of the dip distribution over the four intervals

### 3.3 Length distribution

Fig. 9 shows a logarithmic histogram of the length of the dips. Most dips are at the lower boundary of the criterion with a length of 1 s while the longest dip has a duration of 117 s. It is possible that some of the short time events are due to source variability, but it is difficult to distinguish between absorption dipping and source variability at short time scales. Therefore dipping events shorter than 1 s are excluded from the beginning (see section 2.3). There might be an overestimation of short dips but an objective, formal criterion which is transparent was preferred over the subjective excluding of dips. However the long timescale events could be clearly identified as dipping events.

It is obvious that longer dips are far more rare than short ones. Looking at some of the longer dips one gets the impression that they have substructures and that there is a possibility that they consist of several shorter dips. This would explain the partial covering described by Bałucińska-Church et al. (2000) as being partial covered in time and therefore due to insufficient time resolution. Which is more convincing than a spatial partial covering model because of the small extension the of the source.

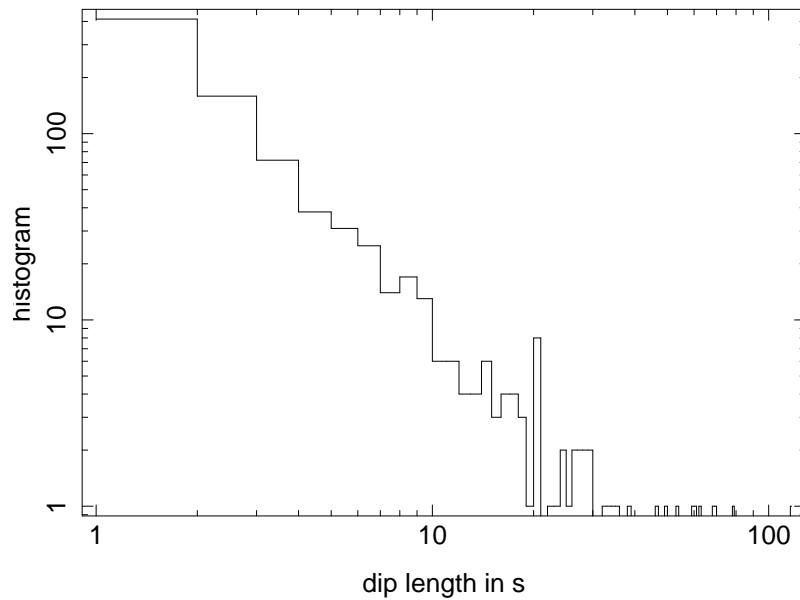


Figure 9: Logarithmic histogram of the dip length

## 4 Summary and outlook

The aim of this work was to study absorption dips in RXTE data from Cyg X-1. First a criterion was found based on the deviation of the hardness ratio from the local mean. This criterion turned out to work in the hard state of the source while not only indicating dips during the soft state.

A distribution of dips in hard state over the orbital period was gained. It showed that dips only occur near superior conjunction of the black hole. This is in contrast to the orbital distribution seen in earlier works, where a fixed value for the hardness ratio was used as a criterion. While the distribution seems to be statistically stable it seems to evolve in time. This time evolution in the dip distribution cannot be due to faults in the ephemeris. Studying the length distribution of dips showed that longer dips which have duration up to 100s are less frequent than shorter ones. There is a possibility that long dips consist of a series of short dips.

To obtain a better understanding of dipping a criterion which is able to find dips in the soft state would be helpful. This should take into account the count rates because of the problems discussed in Section 2.3.

Furthermore the time evolution of the dip distribution should be investigated further as this could yield information about what causes dipping. In addition a distribution of dip length with orbital phase may help answering the question if longer dips are only a sample of shorter dips and so give new information for the question of partial covering.

## List of Figures

1	Monthly exposure . . . . .	3
2	Hardness-intensity-diagram . . . . .	4
3	Typical dipping event in the hard state . . . . .	5
4	Typical dipping event in the soft state . . . . .	6
5	Distribution of the hard dips over the orbital period . . . . .	7
6	Subsets of the dip distribution (every other dataset) . . . . .	8
7	Subsets of the dip distribution (first/second half) . . . . .	8
8	Temporal evolution of the dip distribution . . . . .	10
9	Length distribution . . . . .	11

## List of Tables

1	Used PCA-channels and corresponding energy in PCA epoch 5 . . . . .	3
2	Duration of the four intervals . . . . .	9

## References

- Bałucińska-Church M., Church M.J., Charles P.A., et al., 2000, MNRAS 311, 861
- Jahoda K., Markwardt C.B., Radeva Y., et al., 2006, ApJS 163, 401
- Kitamoto S., Miyamoto S., Tanaka Y., et al., 1984, PASJ 36, 731
- Poutanen J., Zdziarski A.A., Ibragimov A., 2008, MNRAS 389, 1427
- Remillard R.A., McClintock J.E., 2006, ARA&A 44, 49
- Shaposhnikov N., Titarchuk L., 2007, ApJ 663, 445